Order-Parameter Textures and Boundary Conditions in Rotating Vortex-Free ^{3}He-B

J. S. Korhonen,[1] A. D. Gongadze,[2] Z. Janú,[1,a] Y. Kondo,[1] M. Krusius,[1] Yu. M. Mukharsky,[3] and E. V. Thuneberg[4]

[1]*Low Temperature Laboratory, Helsinki University of Technology, 02150 Espoo, Finland*
[2]*Institute of Physics, Georgian Academy of Sciences, 380077 Tbilisi, U.S.S.R.*
[3]*Institute for Physical Problems, Academy of Sciences, 117334 Moscow, U.S.S.R.*
[4]*Research Institute for Theoretical Physics, University of Helsinki, 00170 Helsinki, Finland*

(Received 16 April 1990; revised manuscript received 13 August 1990)

The order-parameter texture has been studied in rotating ^{3}He-B in the vortex-free state with NMR techniques. A sequence of textural phase transitions is observed with increasing rotation speed. It is generated by competing interactions with magnetic field, surfaces, and rotation. Two surface interactions are extracted: the susceptibility anisotropy at the wall and the gyromagnetism due to a magnetic-field–induced surface supercurrent. The results are consistent with an order-parameter structure approaching the planar state with diffuse quasiparticle scattering at the wall.

PACS numbers: 67.50.Fi

It is well known that superfluids respond to rotation by nucleating quantized vortex lines. However, in superfluid ^{3}He-B the nucleation process can be suppressed.[1] This results in a counterflow $(\mathbf{v}_s - \mathbf{v}_n)$ of the stationary superfluid $(\mathbf{v}_s = 0)$ and the uniformly rotating normal fluid $(\mathbf{v}_n = \boldsymbol{\Omega} \times \mathbf{r})$. Counterflow velocities of 1 cm/s or more can be reached, which is a sizable fraction of the Landau pair-breaking velocity $\Delta(0)/p_F = 3$–7 cm/s. The superflow now becomes the dominant orienting mechanism in the order-parameter texture.

We have observed in the vortex-free state four distinctly different types of NMR line shapes as a function of the rotation velocity Ω. Numerical calculations of the order-parameter textures have been employed to reproduce the line shapes. Comparing measurement to calculation, we identify the three transitions separating the four textures as being, in one case, a first-order transition and, in two cases, rounded vestiges of second-order transitions in the limit of a sample cylinder with infinite radius R.

The counterflow velocity is highest at the cylindrical container wall and thus efficient use can be made of the vortex-free textures to probe the textural surface interactions. We extract both the susceptibility anisotropy and gyromagnetism due to the inhomogeneous order-parameter distribution at the surface. The results are consistent with our Ginzburg-Landau calculation of the order-parameter structure at the wall assuming (1) diffuse quasiparticle scattering and (2) a surface structure approaching the planar state, as was first implied by Ambegaokar, de Gennes, and Rainer.[2] The latter finding is in contradiction with a recent interpretation[3] of rotational asymmetry observed in the first measurements on the rotating vortex-free state in Ref. 1.

The NMR measurements have been conducted using a fixed-frequency cw spectrometer at 0.9 and 1.8 MHz. To sustain the vortex-free counterflow, the NMR sample is isolated from finely divided material, such as the sintered heat exchanger, by a long channel and an orifice of 0.5 mm diameter. With this setup faster vortex-free rotation can be obtained than before and vortices seem to reach the sample volume mainly by leaking through the orifice. Using empirically developed recipes one may form either vortex or counterflow states or their combinations. These can be distinguished from their NMR signatures.

Our experimental cell is a cylinder in axial magnetic field and rotation, similar to that in Ref. 1, but, instead of a long cylinder, we use one with diameter = height = 7 mm. Comparing our NMR spectra to those in Ref. 1, one finds that the short cylinder supports a single-domain flare-out texture[4] of lower homogeneity. In a long cylinder the texture generally precipitates with stationary solitonlike defects, which leave their distinct signature in the NMR spectrum. Thus the top and bottom plates, which perturb the ideal cylindrical geometry, act favorably in stabilizing the texture in the short cylinder: This reduces the number of competing, energetically nearly degenerate states and allows us to focus on the more important Ω-dependent events.

The B phase is described in terms of a rotation matrix $\vec{R}(\Theta = \arccos(-\frac{1}{4}), \hat{\mathbf{n}})$. The texture problem[4] consists of the task of finding the spatial distribution of the rotation axis $\hat{\mathbf{n}} = (-\hat{\mathbf{r}}\cos\alpha + \hat{\boldsymbol{\phi}}\sin\alpha)\sin\beta + \hat{\mathbf{z}}\cos\beta$. The three main interactions orienting $\hat{\mathbf{n}}$ are (1) the magnetic-field energy $F_H = -a\int d^3r(\hat{\mathbf{n}}\cdot\mathbf{H})^2$, (2) the flow energy $F_v = -(2a\Omega^2/5v_D^2)\int d^3r\, r^2(\mathbf{H}\cdot\vec{R}\cdot\hat{\boldsymbol{\phi}})^2$, and (3) the surface energy $F_S = -d\int d^2r(\mathbf{H}\cdot\vec{R}\cdot\hat{\mathbf{r}})^2$. Here the dipolar flow velocity v_D gauges the scale of the dipolar energy. The three interactions are in conflict: F_H favors $\hat{\mathbf{n}}$ parallel to $\mathbf{H}$ $(\beta = 0)$; F_v and F_S both favor the polar angle $\beta = 63.4°$ or $180° - 63.4° = 116.6°$, but they disagree in the azimuthal angle α by 90°. This is the origin of the textural transitions. The bending of $\hat{\mathbf{n}}$ is limited by the gradient energy F_G and is characterized by the long magnetic coherence length $\xi_H \sim 0.1$–1 mm. We idealize

the NMR cell as an infinitely long cylinder. All the axially symmetric flare-out textures are fourfold degenerate, generated by the symmetry transformations $(\alpha,\beta) \rightarrow (\alpha+\pi,\beta)$, $(\alpha,\beta) \rightarrow (-\alpha,\pi-\beta)$, and $(\alpha,\beta) \rightarrow (\pi-\alpha, \pi-\beta)$. We choose to describe one of them having $\beta(r=0)=0$. In the limit $R,d/a \gg \xi_H$, there are 32 locally stable textures of which eight are nondegenerate. As a function of Ω there are four global minimum-energy configurations which will be described next.

Volovik and Mineev[5] have proposed that there exists a small gyromagnetic surface energy, $F_{gm}=(2a\kappa R\Omega/5)\int d^2r(\mathbf{H}\cdot\vec{\mathbf{R}}\cdot\hat{\mathbf{z}})$, which arises from a slight deviation of the order parameter from $\vec{\mathbf{R}}(\Theta,\hat{\mathbf{n}})$ caused by particle-hole asymmetry in a magnetic field. This deviation and the suppression of the order parameter near surfaces couple to generate a surface current, an associated angular momentum $\mathbf{L}$, and an energy term $F_{gm}=-\boldsymbol{\Omega}\cdot\mathbf{L}$. For comparison, the larger F_S term arises from the susceptibility anisotropy near surfaces, and is proportional to the gap anisotropy, $d \propto \int dr(\Delta_\parallel^2-\Delta_\perp^2)$.

The NMR absorption signals in Fig. 1 are analyzed using the local oscillator model: The normalized frequency shift from the Larmor value is approximately proportional to $\sin^2\beta(r)$. A plateau in the $\beta(r)$ distribution is seen as a maximum in the absorption line. The signal on the bottom ($\Omega=0.22$ rad/s) corresponds to the *simple flare-out texture*.[4] The peak above the Larmor edge ($\beta=0$) comes from the $\beta\sim0$ plateau in the center of the cylinder. At larger radii, $\hat{\mathbf{n}}$ bends monotonically towards its surface orientation $\beta(R)=\beta_S \leq 63.4°$. This produces the absorption tail which extends to the end point $\sin^2\beta_S$ and then falls off as dictated by the natural linewidth. This texture, in which α roughly equals the wall-preferred value 60° everywhere, remains essentially unchanged at small Ω except for the slight asymmetry displayed in Fig. 2.

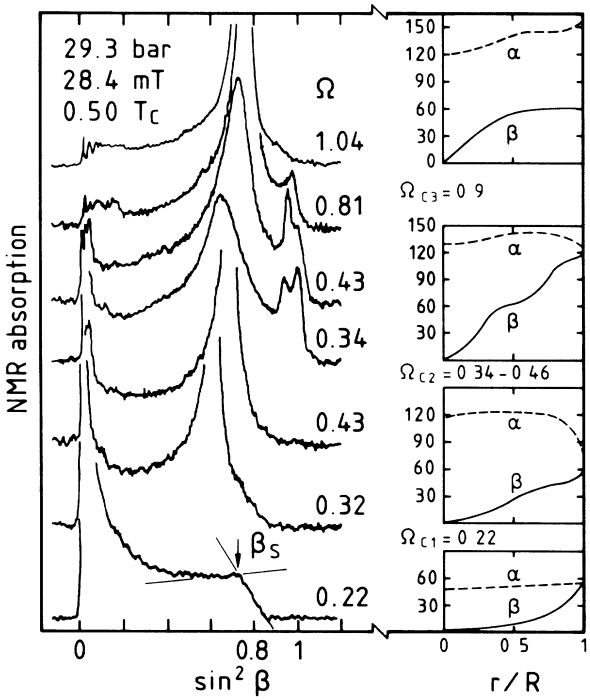

FIG. 1. NMR absorption signals of flare-out textures in vortex-free rotation, plotted vs normalized frequency shift $\sin^2\beta$ and stacked in order of increasing Ω. On the right-hand side are the characteristic radial distributions of the azimuthal angle α and the polar angle β of the order-parameter axis $\hat{\mathbf{n}}$ for the four axially symmetric counterflow textures, separated by three critical velocities Ω_{ci}. From bottom to top: *simple, parted, extended, and crowned flare-out textures.*

On further increasing Ω, a simple analysis of the textural energies in a large cylinder $R \gg \xi_H$ gives a second-order transition at $\Omega_{c1}=v_D/R$. Our numerical calculation shows that this transition becomes rounded in a cylinder of finite size but remains identifiable as an abrupt change in the angle α: It now becomes roughly equal to the flow-dominated value 150° over much of the cross section except near the wall where it approaches the wall-dominated value 60°. The new texture is called the *parted flare-out texture* as there exists in the r-ϕ plane a circular partition line which divides the texture into regions with $\hat{\mathbf{n}}$ oriented inward and outward. The transition to this texture is clearly observed in the NMR line shape: (1) The large counterflow absorption peak, characteristic for the vortex-free state, starts to build up (see $\Omega \geq 0.32$ rad/s in Fig. 1), and (2) there is a change in the slopes of both $\sin^2\beta_S$ (see Fig. 2) and the spin-wave eigenfrequencies (see Ref. 1) as a function of Ω.

With increasing Ω the counterflow peak grows into a sharp line, which may split into a double peak, until it loses its narrow width at Ω_{c2} (upper trace at $\Omega=0.43$ in Fig. 1). Like all sudden changes in the texture, the transition is completed on a time scale <1 s. The change signals a first-order transition, now to the *extended flare-out texture* in which the β distribution $[\beta(0),\beta_S]$ is

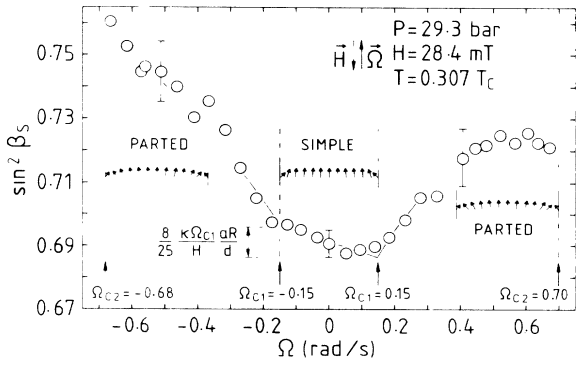

FIG. 2. Normalized frequency shift $\sin^2\beta$ of the high-frequency-signal end point at $\beta(r=R)=\beta_S$ as a function of Ω. The asymmetry with respect to the direction of rotation is explained by surface gyromagnetism and is reversed on inverting the orientation of $\mathbf{H}$. Inset: The projection of $\hat{\mathbf{n}}$ on the r-z plane in the two textures.

extended from $[0, \approx 63.4°]$ to $[0, \approx 116.6°]$. The new end point corresponds to another minimum of F_S: $\beta = 116.6°$ and $\alpha = 120°$. In addition to its extended range of frequency shifts, a second experimental identification mark of the extended texture is a small subsidiary absorption peak (traces $\Omega = 0.43$ and 0.81 in the top part of Fig. 1).

In Fig. 3 measurements of Ω_{c2} are shown; the data fall in two bands separated by a hysteretic region in which either texture may exist depending on how one has moved along the Ω axis. At low Ω in the hysteretic regime the NMR spectrum in the extended texture acquires a new absorption peak at $\beta = 90°$ (trace $\Omega = 0.34$ in Fig. 1). This feature allows us to calibrate the frequency axis in terms of β. In Fig. 3 the measured Ω_{c2} is also compared to the textural calculation, using experimental values of the textural parameters.[6] The agreement is excellent considering that no adjustable parameters have been used and that the approximation of rigid boundary conditions has been applied ($F_S \to \infty$) which gives a lower estimate for Ω_{c2}.

When Ω is increased well beyond Ω_{c2}, ultimately the flow dominates over the surface energy and the main counterflow plateau in $\beta(r)$ expands up to the wall. In this *crowned flare-out texture* $\hat{\mathbf{n}}$ is oriented along $\hat{\mathbf{z}}$ only in the very center of the cylinder, forming a well outlined island or crown in an otherwise homogeneous surrounding with β approaching 63.4°. As in the case of Ω_{c1}, we conclude this to be a smoothed vestige of a second-order transition at Ω_{c3} in the limit $R \gg \xi_H$. In the NMR spectra the subsidiary peak is observed to disappear on accelerating past Ω_{c3}.

The rotating vortex-free state provides an efficient environment for the measurement of the surface interactions. For this one needs to identify in the NMR spectrum the locations of $\beta = 0$ and 90°, in addition to β_S, at each temperature and pressure. In contrast to the parallel-plate geometry ($F_G \to \infty$),[7,8] in the open volume $\beta = 0$ and 90° are well defined while β_S is blurred by the natural linewidth broadening superimposed on the $\beta(r)$ distribution. We determine β_S from the absorption maximum in the tail of the signals when $\Omega < \Omega_{c2}$ (see Fig. 1). This convention gives a lower bound which improves in precision the sharper the maximum gets with increasing ξ_H. One finds that $\sin^2\beta_S$ is a smooth and monotonous function which increases with decreasing temperature and pressure.

We extract the surface length d/a from the measured $\sin^2\beta_S$ by using a numerical calculation of $\sin^2\beta_S$ as a function of $a\xi_H/d$ and R/ξ_H. In Fig. 4 the results are compared with a Ginzburg-Landau calculation of the order parameter near a wall. The latter d/a values have the temperature dependence $(1 - T/T_c)^{1/2}$, are based on the order parameter approaching the planar state,[9] and are shown here for both the diffuse and specular limits of quasiparticle scattering from the wall. We conclude that the measurements extrapolate within the combined uncertainties to the calculated results in the diffuse limit,

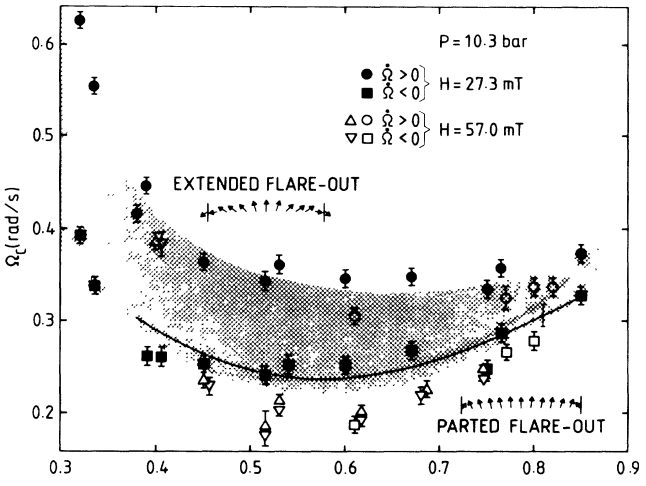

FIG. 3. Critical rotation velocity Ω_{c2} for the transition from the *parted* to the *extended flare-out texture* during accelerating rotation (upper branch) and for the reverse transition during decelerating rotation (lower branch), plotted vs temperature. The two branches are separated by a hysteretic (hatched) region. The solid line represents the calculated Ω_{c2} for which the energies of the two textures are equal, assuming rigid boundary conditions. Ω_{c2} is nearly independent of H: With the exception of the gradient energy all relevant interactions scale as H^2.

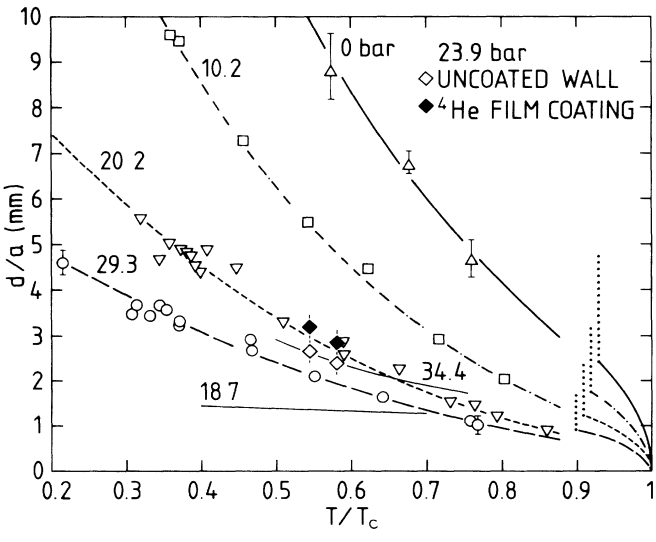

FIG. 4. The surface length d/a vs temperature at different pressures. The measurements at 18.7 bars are from Ref. 7 and at 34.4 bars from Ref. 8. The curves close to T_c correspond to Ginzburg-Landau calculations for the planar surface structure in the diffuse scattering limit. The dotted vertical lines denote the range of change of these curves if the scattering is changed from diffuse (bottom) to specular (top).

but fall below those in the specular limit. This conclusion is consistent with other experiments, such as the suppression of T_c in confined geometries whose dimensions approach the superfluid coherence length ξ_0. By coating the walls with a superfluid ^{4}He film, d/a is expected to increase closer to the specular scattering limit. As shown in Fig. 4, this is indeed the case, if one compares the results for the uncoated NMR cell to those with a saturated ^{3}He/^{4}He film lining. We conclude that the uncoated epoxy cell constitutes an environment in which the walls are rough on the scale of quasiparticle scattering but not on the scale of vortex nucleation.

An asymmetry with respect to the direction of rotation becomes discernible below $0.5T_c$ in $\sin^2\beta_S$ and in the critical velocity Ω_{c2}. Since the asymmetry changes sign by inverting the direction of **H**, we interpret the effect as gyromagnetism. We find that the parameter κ is positive and increases with decreasing temperature and pressure. From Fig. 2 one obtains $\kappa \approx 5$ mTs/rad with $\pm 50\%$ uncertainty while its Ginzburg-Landau estimate, based on the planar-surface structure, is -0.08 in the diffuse and -0.19 in the specular limits. This difference may not represent a disagreement since the temperature regimes of the two results do not overlap. The vortex-core gyromagnetism is known to display similar strong pressure and temperature dependences with possibly a change in sign in the latter.[6] We note that both κ and d/a are roughly twice as large in the specular limit than in the diffusive limit. A result for κ, falling between these limiting cases, was found earlier by Volovik and Mineev[5] using a boundary-condition-independent model for the order parameter.

In the earlier vortex-free experiment[1] the asymmetry between rotation directions was much larger than in the present one, and it was also observed at high temperatures. Moreover, its sign did not correlate with the magnetic field, so that it cannot be explained by gyromagnetism. Calculations[9] in the Ginzburg-Landau limit indicate that, with bulk ^{3}He-B in the container, the walls may become coated with an A-state surface layer at high pressures and high rotation velocities in the presence of specular quasiparticle scattering. On this basis it was proposed[3] that the rotational asymmetry can be understood in terms of a phase transition in the surface structure from planar to A when warming through $T \sim 0.4T_c$. However, in spite of extensive variation in the experimental procedure or the externally controllable parameters, we were not able to induce a discontinuity in $\sin^2\beta_S$ which would signal a transition in the surface structure. It is interesting to note that F_S has two extrema, namely, $\beta = 63.4°$ and 0. For the planar surface structure the former orientation corresponds to minimum energy and the latter to a maximum. For the A surface structure the character of the extrema is reversed in the Ginzburg-Landau regime for $\Omega < 0.5$ rad/s. Thus the boundary condition for the A structure is dramatically different because $\hat{\mathbf{n}}$ is allowed to remain parallel to **H** even at the wall and the flare-out texture would be absent. While this conclusion is not guaranteed beyond the Ginzburg-Landau regime it is still in contradiction with all experimental evidence. We conclude that the large asymmetry in Ref. 1 is caused by some still unidentified textural irregularity.

In summary, we have observed a sequence of textural phase transitions in rotating vortex-free ^{3}He-B in agreement with calculation. The textural boundary conditions are both measured and calculated, and reasonable agreement is found with diffuse boundary scattering and an order-parameter structure approaching the planar state at the surface. A gyromagnetic contribution to the textural energy has been identified which is interpreted to arise from a magnetic-field-induced surface current and, according to calculation, also depends within a factor of 2 on the nature of quasiparticle scattering.

We wish to thank V. Ambegaokar, P. Hakonen, G. Kharadze, O. Lounasmaa, V. Mineev, M. Salomaa, E. Sonin, and G. Volovik. This work has been supported by the Körber Stiftung.

[a]Present address: Institute of Physics, Academy of Sciences, 18040 Prague 8, Czechoslovakia.

[1]P. J. Hakonen and K. K. Nummila, Phys. Rev. Lett. **59**, 1006 (1987).

[2]V. Ambegaokar, P. G. de Gennes, and D. Rainer, Phys. Rev. A **9**, 2676 (1974).

[3]M. M. Salomaa and G. E. Volovik, J. Low Temp. Phys. **75**, 209 (1989).

[4]H. Smith, W. F. Brinkman, and S. Engelsberg, Phys. Rev. B **15**, 199 (1977).

[5]G. E. Volovik and V. P. Mineev, Zh. Eksp. Teor. Fiz. **86**, 1667 (1984) [Sov. Phys. JETP **59**, 972 (1984)].

[6]P. J. Hakonen *et al.*, J. Low Temp. Phys. **76**, 225 (1989); K. K. Nummila *et al.*, Europhys. Lett. **9**, 355 (1989).

[7]A. I. Ahonen, M. Krusius, and M. A. Paalanen, J. Low Temp. Phys. **25**, 421 (1976).

[8]D. D. Osheroff, Physica (Amsterdam) **90B**, 20 (1977).

[9]E. V. Thuneberg, Phys. Rev. B **33**, 5124 (1986).

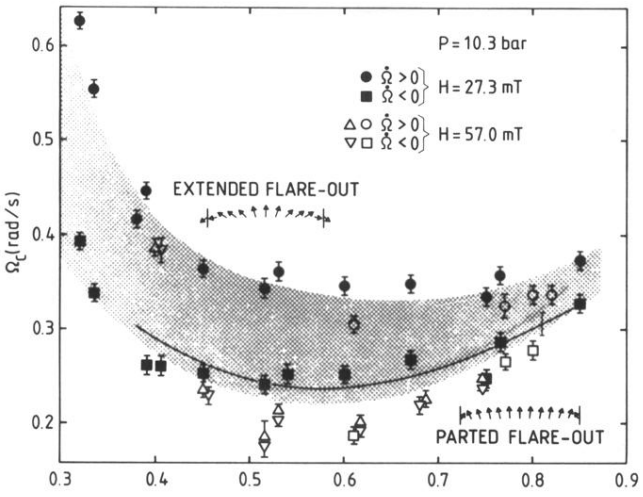

FIG. 3. Critical rotation velocity Ω_{c2} for the transition from the *parted* to the *extended flare-out texture* during accelerating rotation (upper branch) and for the reverse transition during decelerating rotation (lower branch), plotted vs temperature. The two branches are separated by a hysteretic (hatched) region. The solid line represents the calculated Ω_{c2} for which the energies of the two textures are equal, assuming rigid boundary conditions. Ω_{c2} is nearly independent of H: With the exception of the gradient energy all relevant interactions scale as H^2.